**Article ID:** 1000-324X(2016)11-1258-05 **DOI:** 10.15541/jim20160135

# Wide Bandgap Engineering of β-(Al, Ga)$_2$O$_3$ Mixed Crystals

XIAO Hai-Lin[1, 2], SHAO Gang-Qin[3], SAI Qing-Lin[1], XIA Chang-Tai[1], ZHOU Sheng-Ming[1], YI Xue-Zhuan[1]

(1. Key laboratory of Materials for High Power Laser, Shanghai Institute of Optics and Fine Mechanics, Chinese Academy of Sciences, Shanghai 201800, China; 2. University of Chinese Academy of Sciences, Beijing 100049, China; 3. State Key Laboratory of Advanced Technology for Materials Synthesis and Processing, Wuhan University of Technology, Wuhan 430070, China)

**Abstract:** Bandgap tunable β-(Al, Ga)$_2$O$_3$ mixed crystals with different $Al^{3+}$ concentration were grown by the optical floating zone (OFZ) method. When the nominal $Al^{3+}$ doping concentration was close to 0.26, cracking appeared. The powder X-ray diffraction (XRD) revealed that β-(Al, Ga)$_2$O$_3$ mixed crystals kept the crystal structure of β-Ga$_2$O$_3$ without foreign phases and the lattice parameters decreased with the increasing $Al^{3+}$ concentration. $^{27}$Al magic angle spinning (MAS) nuclear magnetic resonance (NMR) spectroscopy showed that $Al^{3+}$ occupied $Ga^{3+}$ positions and the ratio of $Al^{3+}$(IV)/ $Al^{3+}$(VI) was about 1:3. The transmittance spectra were measured to investigate the bandgap of β-(Al, Ga)$_2$O$_3$ mixed crystals. Results showed that the bandgap increased continuously with the $Al^{3+}$ concentration increasing from 4.72 eV to 5.32 eV, which may extend the application of β-Ga$_2$O$_3$ crystal in optoelectronic devices operating at shorter wavelength.

**Key words:** β-Ga$_2$O$_3$; $Al^{3+}$; bandgap; semiconductors

According to Geller[1], the crystalline-structure of beta gallium oxide (β-Ga$_2$O$_3$) belongs to the monoclinic system with a base centered space group C2/m and the lattice parameters are $a$=1.2214 nm, $b$=0.30371 nm, $c$= 0.57981 nm and β=103.83°[2]. The bandgap of β-Ga$_2$O$_3$ is about 4.8 eV, making it transparent from deep ultra violet (DUV) to infrared region (IR), where the cutoff wavelength is about 260 nm. The crystalline β-Ga$_2$O$_3$ is of high chemical and physical stabilities. The high quality and large-size single-crystalline β-Ga$_2$O$_3$ bulk substrates can be obtained through simple and low-cost melt growth methods such as optical floating zone method[3], edge-defined film fed growth (EFG) method[4] and Czochralski method[5-6], which has positioned it as a strong candidate for next generation optoelectronic devices operating at shorter wavelength such as ultraviolet transparent electrodes[7], photodetectors[8-9], conductive windows[10], field-effect transistors (FETs)[11] and also high temperature oxygen sensors[12-14]. However, all of these achievements should have a premise: the bandgap engineering. Tunable bandgap is highly desired because it allows great flexibility in designing and optimizing these devices. By doping indium and aluminum, Zhang, *et al*[15-16] and other authors[17-19] have reported bandgap tunable (Ga, In)$_2$O$_3$ and (Al, Ga)$_2$O$_3$ films. But there are no other articles which report the bandgap tunable β-Ga$_2$O$_3$ crystals. In this paper, β-(Al, Ga)$_2$O$_3$ mixed crystals with different $Al^{3+}$ concentrations were grown by the floating zone technique and their crystal structure and transmittance spectra are investigated.

## 1 Experimental

### 1.1 Crystals growth and processing

β-(Al, Ga)$_2$O$_3$ mixed crystals were grown by the optical floating zone (OFZ) method. β-Ga$_2$O$_3$ powder with grade of 5N (99.999%) purity was used as the starting material, and mixed in mortar with Al$_2$O$_3$ powder (purity 99.999%). The nominal $Al^{3+}$ concentration (mole ratio of Al/(Al+Ga)) in the mixed powder is $x_p$= 0.09, 0.17, 0.23, 0.26. The feed rods were pressed by traditional ceramic processes. These mixed powders were compressed by cold isostatic pressing under a pressure of 210 MPa for 2 min and subsequently sintered at 1500℃ for 20 h in dry air. The sintered rods were about 70–80 mm long and 6–7 mm in diameter. β-(Al, Ga)$_2$O$_3$ mixed crystals were grown by the optical floating zone technique using a Quantum Design IRF01-001-00 infrared image furnace. The speed of the

**Received date:** 2016-03-09; **Modified date:** 2016-03-30
**Foundation item:** Science and Technology Commission of Shanghai Municipality (13111103700)
**Biography:** XIAO Hai-Lin(1989–), male, candidate of master degree. E-mail: hlxiao2014@163.com
**Corresponding author:** XIA Chang-Tai, professor. E-mail: xia_ct@siom.ac.cn; SAI Qing-Lin, assistant professor. E-mail: saiql@siom.ac.cn

crystal growth was 5 mm/h, and the rotation of the seed crystal and feed rod was 15 r/min in opposite directions. The crystal were grown under the dry air flow with a rate of 0.2 $m^3$/h. Annealingat 1100℃ for 32 h were carried out for the samples in air. After annealing, the samples were cooled down to room temperature slowly and cut along (100) plane. The samples were mechanically polished into 0.4 mm-thick wafers parallel to β-(Al, $Ga)_2O_3$ (100) plane.

### 1.2 Characterizations

The concentration of $Al^{3+}$ in the mixed crystals was determined by PerkinElmer 7300Dv inductively coupled plasma (ICP) atomic emission spectrometry. The structure of the mixed crystals were examined by conventional $\theta$-$2\theta$ X-ray diffraction (XRD, Ultima IV Diffractometer, Rigaku, Japan) using Cu $K_\alpha$ emission line (λ=0.154060 nm, 40 kV, 40 mA). $^{27}$Al MAS-NMR spectra were carried out on Bruker Avance-500 spectrometer at the magnetic field strengths of 11.7 and 7.04 T, using a 4 mm rotor. The resonance frequency is 14 kHz, using pulse length of 1.0 μs (30° solid pulse length) and relaxation time of 1 s. The structure refinement was performed by Rietvld method with GSAS/EXIGUI software. Optical transmittance spectra were measured with a PerkinElmer Lambda 750 UV/VIS/NIR spectrometer at room temperature.

## 2 Results and discussion

The β-(Al, $Ga)_2O_3$ mixed crystals doped with different $Al^{3+}$ concentrations are shown in Fig. 1. The crystals are colorless and transparent. The size of them is about 35 mm in length and 6 mm in diameter. When the nominal doping $Al^{3+}$ concentration is about 0.26, cracking appears.

The $Al^{3+}$ concentration in mixed crystal detected by ICP ($x$) *versus* $Al^{3+}$ concentration in mixed powder ($x_p$) is displayed in Fig. 2. The concentration of $Al^{3+}$ in the mixed crystals is greater than the nominal concentration, which is due to the volatilization of $Ga_2O_3$. The experimental results can be fitted by a linear function $x = 1.33x_p$. From this function, we can see that the concentration of $Al^{3+}$ in mixed crystals linearly scale up with the nominal $Al^{3+}$ doping concentration in mixed powders. The results indicate that desired compositional β-(Al, $Ga)_2O_3$ mixed crystals can be obtained easily through changing the $Al^{3+}$ concentration in mixed powders, making it possible to design β-(Al, $Ga)_2O_3$ based devices as the microstructures and properties of semiconductor materials strongly depend on the composition.

Figure 3(a) shows the powder XRD patterns of β-$(Al_xGa_{1-x})_2O_3$ ($x$ = 0, 0.12, 0.31) mixed crystals. Fig. 3(b) is the final observed, calculated and difference profiles for

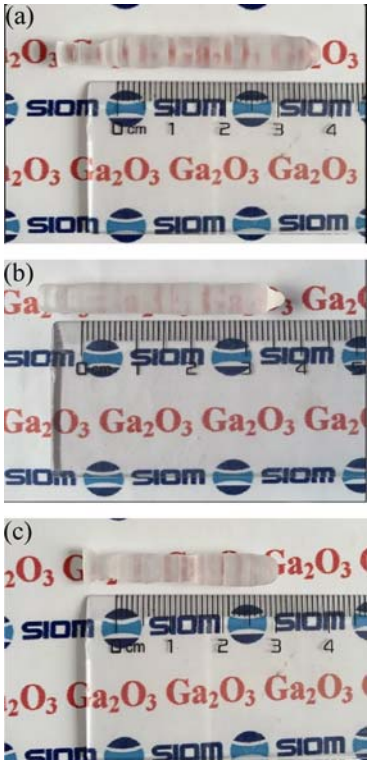


Fig. 1 Pictures of β-(Al, $Ga)_2O_3$ mixed crystal ingots doped with different Pictures of $Al^{3+}$ concentrations
(a) 0.09; (b) 0.17; (c) 0.23

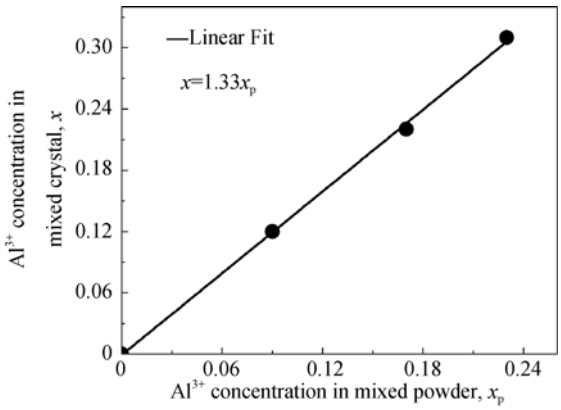


Fig. 2 $Al^{3+}$ concentration in mixed crystal $x$ *vs* $Al^{3+}$ concentration in mixed powder $x_p$

Rietveld refinement of the β-$(Al_{0.12}Ga_{0.88})_2O_3$ structure. Results show that pure monoclinic phase with space group of C 12/m 1 (No. 5) have been obtained. The refinement for β-$(Al_xGa_{1-x})_2O_3$ ($x$ = 0, 0.12, 0.31) converged while goodness of fit ($\chi^2$) was 2.67, 7.10 and 10.6, respectively. The refined lattice parameters are listed in Table 1. The lattice parameters of $a$, $b$ and $c$ decrease while β increases a little with the increasing of $Al^{3+}$ concentration, consistent with the experimental report of (Al, $Ga)_2O_3$ film[8]. Thus the volume ($V$) of crystal cells decreases, indicating that the smaller $Al^{3+}$ has occupied the

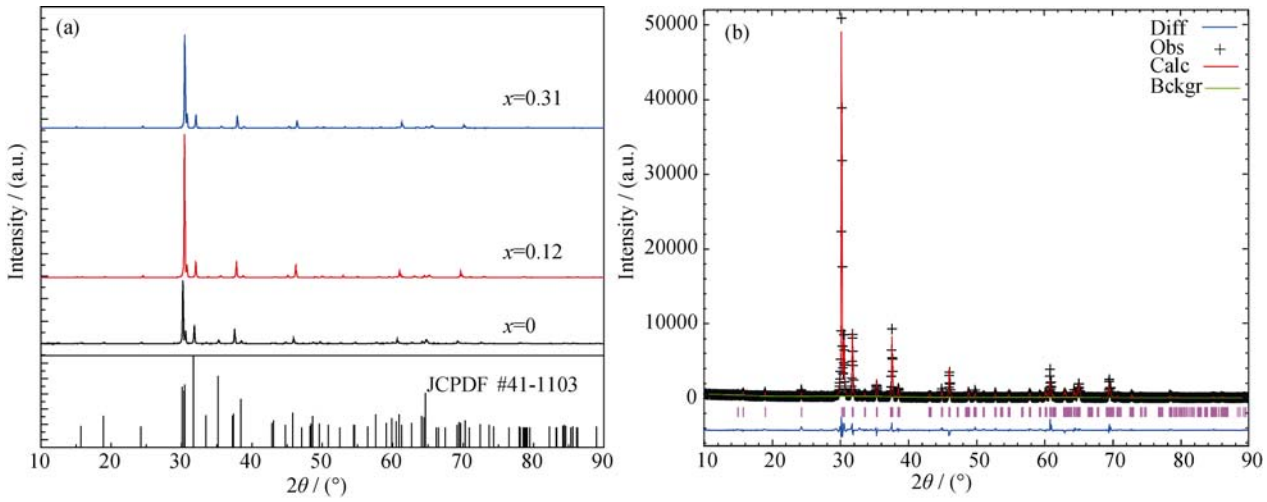


Fig. 3 (a) Powder XRD patterns of $\beta$-$(Al_xGa_{1-x})_2O_3$ ($x$ = 0, 0.12, 0.31) mixed crystals and (b) The final observed, calculated and difference profiles for Rietveld refinement of the β-$(Al_{0.12}Ga_{0.88})_2O_3$ structure

**Table 1 Refined lattice parameters for $\beta$-$(Al_xGa_{1-x})_2O_3$ ($x$ = 0, 0.12, 0.31)**

| | $a$/nm | $b$/nm | $c$/nm | $\beta$ /(°) | $V$/nm$^3$ |
|---|---|---|---|---|---|
| β-$Ga_2O_3$ | 1.22289(3) | 0.303736(16) | 0.580719(19) | 103.842(3) | 0.209436(11) |
| β-$(Al_{0.12}Ga_{0.88})_2O_3$ | 1.21859(2) | 0.302667(18) | 0.579099(18) | 103.917(3) | 0.207316(13) |
| β-$(Al_{0.31}Ga_{0.69})_2O_3$ | 1.21173(4) | 0.30040(3) | 0.57660(3) | 104.003(4) | 0.203646(18) |

crystal position of $Ga^{3+}$ to form mixed crystal structure.

$^{27}$Al MAS NMR spectra of three β-$(Al_xGa_{1-x})_2O_3$ ($x$ = 0, 0.12, 0.31) mixed crystal samples are shown in Fig. 4. The NMR spectra show well-resolved octahedral and tetrahedral Al sites. Octahedrally coordinated Al are found in δ=5-20 and tetrahedrally coordinated Al in δ=48-47. The amount of Al in octahedral position is larger than that in tetrahedral position. The reason is that the total energy of β-(Al, Ga)$_2$O$_3$ is more higher in the case of $Al^{3+}$ occupying the tetrahedral $Ga^{3+}$ sites[20]. After integrating the peak intensities, we find that the ratio of $Al^{3+}$(IV)/ $Al^{3+}$(VI) is about 1:3.

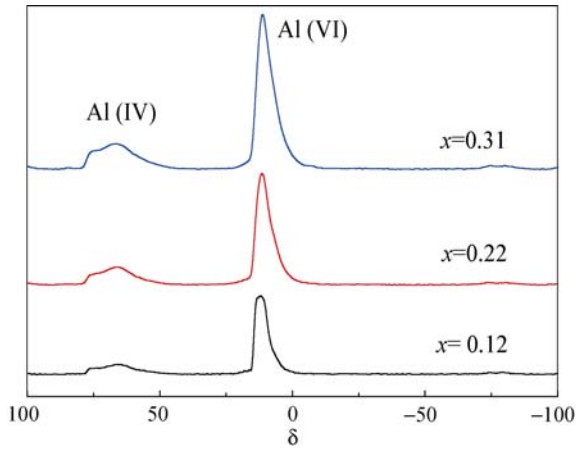


Fig. 4 $^{27}$Al MAS NMR spectra of series β-$(Al_xGa_{1-x})_2O_3$ ($x$= 0.12, 0.22, 0.31) samples

The transmittance spectra of β-(Al, Ga)$_2$O$_3$ mixed crystals with different $Al^{3+}$ concentrations ($x$) is shown in Fig. 5. A sharp absorption edge which is caused by the fundamental absorption of light for β-(Al, Ga)$_2$O$_3$ mixed crystal is observed. Those absorption edges shift to shorter wavelength from 255 nm to 228 nm with the increasing of $Al^{3+}$ concentration $x$. The bandgap of the β-(Al, Ga)$_2$O$_3$ mixed crystals, as shown in the insertion of Fig. 5, can be obtained by extrapolating the linear part of $(\alpha h\upsilon)^2$~$h\upsilon$ to the horizontal axis. Here, $h\upsilon$ is the energy of the incident photon, $\alpha$ is the absorption

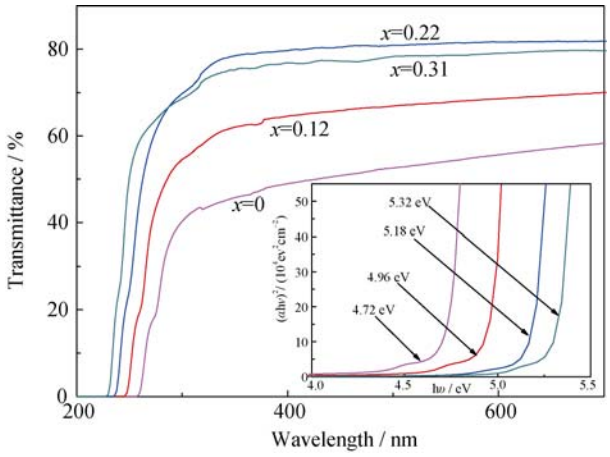


Fig. 5 Transmittance of β-(Al, Ga)$_2$O$_3$ mixed crystals with different $Al^{3+}$concentration in mixed crystals $x$. The insert is $(\alpha h\upsilon)^2$ *vs* $h\upsilon$ plot of β-(Al, Ga)$_2$O$_3$ mixed crystals with different $Al^{3+}$ concentration in mixed crystals $x$

coefficient which can be calculated by the standard relation taking the thickness of the mixed crystals into consideration. The absorption coefficient increases rapidly at the photon energy range 4.72–5.32 eV depending on the $Al^{3+}$ concentration in mixed crystals $x$. The good fit between $(\alpha h\upsilon)^2$~$h\upsilon$ and the straight line indicates that the absorption in this energy region is due to the direct transition[8]. This result is different from the recent research which showed the existence of indirect transition[21-22]. This difference comes from the similar energy of direct and indirect gaps as well as the weakness of the indirect transitions. It is generally recognized that the bandgap ($E_g$) of alloy on doping concentration $x$ can be expressed as[23-24]:

$$E_g\,(\mathrm{eV}) = \mathrm{A}+\mathrm{B}x+\mathrm{C}x^2 \quad (1)$$

Fig. 6 is the dependence of bandgap of β-(Al, $Ga)_2O_3$ mixed crystals on $Al^{3+}$ concentration x, From which we can see that the bandgap of β-(Al, $Ga)_2O_3$ mixed crystals increases continuously with the $Al^{3+}$ concentration Through polynomial fitting, we can get a function relationship:

$$E_g\,(\mathrm{eV}) = -0.88x^2+2.24x+4.72 \quad (2)$$

It shows that the bandgap of β-(Al, $Ga)_2O_3$ mixed crystals could be tuned by the concentration of $Al^{3+}$, which provides a method to design optoelectronic devices based on this crystal material.

## 3 Conclusion

Wide bandgap semiconductors β-(Al, $Ga)_2O_3$ mixed crystals with different $Al^{3+}$ concentrations were grown by the optical floating zone(OFZ) method. Powder XRD patterns and $^{27}Al$ MAS NMR spectra reveal that there are no foreign phases and Al occupies the octahedral and tetrahedral Ga positions with a ratio of about 3:1. The maximum nominal doping concentration of $Al^{3+}$ is about 0.26. The bandgap of β-$Ga_2O_3$ single crystals can be changed from 4.72 eV to 5.31 eV continuously through doping different concentrations of $Al^{3+}$, which provides a method to design optoelectronic devices based on this crystal material.

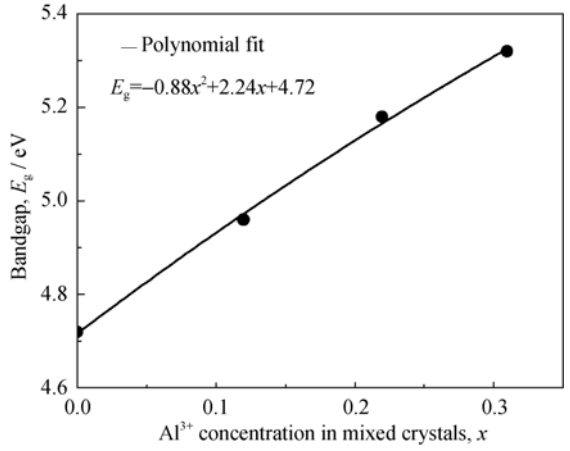


Fig. 6 Bandgap of β-(Al, $Ga)_2O_3$ mixed crystal *vs* $Al^{3+}$ concentration in mixed crystals $x$

## References:


[1] GELLER S. Crystal structure of β-$Ga_2O_3$. *The Journal of Chemical Physics*, 1960, **33(3):** 676–684.

[2] AHMAN J, SVENSSON G, ALBERTSSON J. A reinvestigation of β-gallium oxide. *Acta Crystallographica Section C-Crystal Structure Communications*, 1996, **52(6):** 1336–1338.

[3] VILLORA E G, SHIMAMURA K, YOSHIKAWA K, *et al*. Large-size β-$Ga_2O_3$ single crystals and wafers. *Journal of Crystal Growth*, 2004, **270(3/4):** 420–426.

[4] AIDA H, NISHIGUCHI K, TAKEDA H, *et al*. Growth of β-$Ga_2O_3$ single crystals by the edge-defined, film fed growth method. *Japanese Journal of Applied Physics*, 2008, **47(11):** 8506–8509.

[5] GALAZKA Z, UECKER R, IRMSCHER K, *et al*. Czochralski growth and characterization of β-$Ga_2O_3$ single crystals. *Crystal Research and Technology*, 2010, **45:** 1229–1236.

[6] GALAZKA Z, IRMSCHER K, UECKER R, *et al*. On the bulk β-$Ga_2O_3$ single crystals grown by the Czochralski method. *Journal of Crystal Growth*, 2014, **404:** 184–191.

[7] UEDA N, HOSONO H, WASEDA R, *et al*. Synthesis and control of conductivity of ultraviolet transmitting β-$Ga_2O_3$ single crystals. *Applied Physics Letters*, 1997, **70(26):** 3561–3563.

[8] KOKUBUN Y, MIURA K, ENDO F, *et al*. Sol-Gel prepared β-$Ga_2O_3$ thin films for ultraviolet photodetectors. *Applied Physics Letters*, 2007, **90(3):** 031912-1-3.

[9] OSHIMA T, OKUNO T, ARAI N, *et al*. Vertical solar-blind deep-ultraviolet schottky photodetectors based on β-$Ga_2O_3$ substrates. *Applied Physics Express*, 2008, **1(1):** 011202-1-3.

[10] TOMM Y, KO J M, YOSHIKAWA A, *et al*. Floating zone growth of β-$Ga_2O_3$: a new window material for optoelectronic device applications. *Solar Energy Materials and Solar Cells*, 2001, **66(1–4):** 369–374.

[11] MATSUZAKI K, HIRAMATSU H, NOMURA K, *et al*. Growth, structure and carrier transport properties of $Ga_2O_3$ epitaxial film examined for transparent field-effect transistor. *Thin Solid Films*, 2006, **496(1):** 37–41.

[12] BARTIC M, BABAN C I, SUZUKI H, *et al*. β-gallium oxide as oxygen gas sensors at a high temperature. *Journal of the American*

*Ceramic Society*, 2007, **90(9):** 2879–2884.

[13] OGITA M, YUASA S, KOBAYASHI K, *et al*. Presumption and improvement for gallium oxide thin film of high temperature oxygen sensors. *Applied Surface Science*, 2003, **212:** 397–401.

[14] FLEISCHER M, MEIXNER H. Gallium oxide thin-films - a new material for high-temperature oxygen sensors. *Sensors and Actuators B-Chemical*, 1991, **4(3/4):** 437–441.

[15] ZHANG F B, SAITO K, TANAKA T, *et al*. Wide bandgap engineering of $(GaIn)_2O_3$ films. *Solid State Communications*, 2014, **186:** 28–31.

[16] ZHANG F B, SAITO K, TANAKA T, *et al*. Wide bandgap engineering of $(AlGa)_2O_3$ films. *Applied Physics Letters*, 2014, **105(16):** 162107-1-5.

[17] KAUN S W, WU F, SPECK J S. β-$(Al_xGa_{1-x})_2O_3$/$Ga_2O_3$ (010) heterostructures grown on β-$Ga_2O_3$ (010) substrates by plasma-assisted molecular beam epitaxy. *Journal of Vacuum Science & Technology A*, 2015, **33:** 041508-1-9.

[18] WAKABAYASHI R, OSHIMA T, HATTORI M, *et al*. Oxygen-radical-assisted pulsed-laser deposition of β-$Ga_2O_3$ and β-$(Al_xGa_{1-x})_2O_3$ films. *Journal of Crystal Growth*, 2015, **424:** 77–79.

[19] SCHMIDT-GROUD R, KRANERT C, VON WENCKSTERN H, *et al*. Dielectric function in the spectral range (0.5–8.5) eV of an $(Al_xGa_{1-x})_2O_3$ thin film with continuous composition spread. *Journal of Applied Physics*, 2015, **117:** 165307-1-7.

[20] ZHENG S W, FAN G H, PI H. Study on the electronic sructures and energy band properties of Al-doped β-$Ga_2O_3$. *Journal of Functional Materials*, 2014, **12(45):** 12102–12107.

[21] YAMAGUCHI K. First principles study on electronic structure of β-$Ga_2O_3$. *Solid State Communications*, 2004, **131(12):** 739–744.

[22] HE H Y, BLANCO M A, PANDEY R. Electronic and thermodynamic properties of β-$Ga_2O_3$. *Applied Physics Letters*, 2006, **88(26):** 261904-1-3.

[23] ZHENG S W, FAN G H, ZHANG Y, *et al*. Study on the lattice constants and energy band properties of Be and Ca doped wurtzite ZnO. *Acta Physica Sinica*, 2012, **61(22):** 227101-1-8.

[24] LAURENTI J P, ROENTGEN P, WOLTER K, *et al*. Indium-doped GaAs-a very dilute alloy system. *Physical Review B*, 1988, **37(8):** 4155–4163.

# 混晶 β-$(Al, Ga)_2O_3$ 的禁带调节

肖海林[1,2], 邵刚勤[3], 赛青林[1], 夏长泰[1], 周圣明[1], 易学专[1]

(1. 中国科学院 上海光学机械精密研究所, 强激光材料重点实验室, 上海 201800; 2. 中国科学院大学, 北京 100049; 3. 武汉理工大学 材料复合新技术国家重点实验室, 武汉 430070)

**摘 要:** 通过光学浮区法生长了不同浓度的 β-$(Al, Ga)_2O_3$ 混晶。当 $Al^{3+}$掺杂浓度达到 0.26 的时候, 晶体生长出现开裂现象。进行 X 射线衍射分析, 结果表明所得 β-$(Al, Ga)_2O_3$ 混晶保持了 β-$Ga_2O_3$ 的晶体结构, 晶体没有出现其他杂质相, 并且随着 $Al^{3+}$浓度的增加, 晶格常数 a、b、c 减小, β 角增大; 核磁共振光谱显示 Al 的确进入了 Ga 的格位并且取代了 Ga 的四配位和六配位格位, 两者的比例约为 1: 3。通过测试 β-$(Al, Ga)_2O_3$ 混晶的透过光谱, 得出 β-$(Al, Ga)_2O_3$ 混晶的禁带调节范围为 4.72~5.32 eV, 扩大了 β-$Ga_2O_3$ 晶体在更短波段的光电子探测器方面的应用。

**关 键 词:** β-$Ga_2O_3$; $Al^{3+}$; 禁带宽度; 半导体

**中图分类号:** TN304 **文献标识码:** A